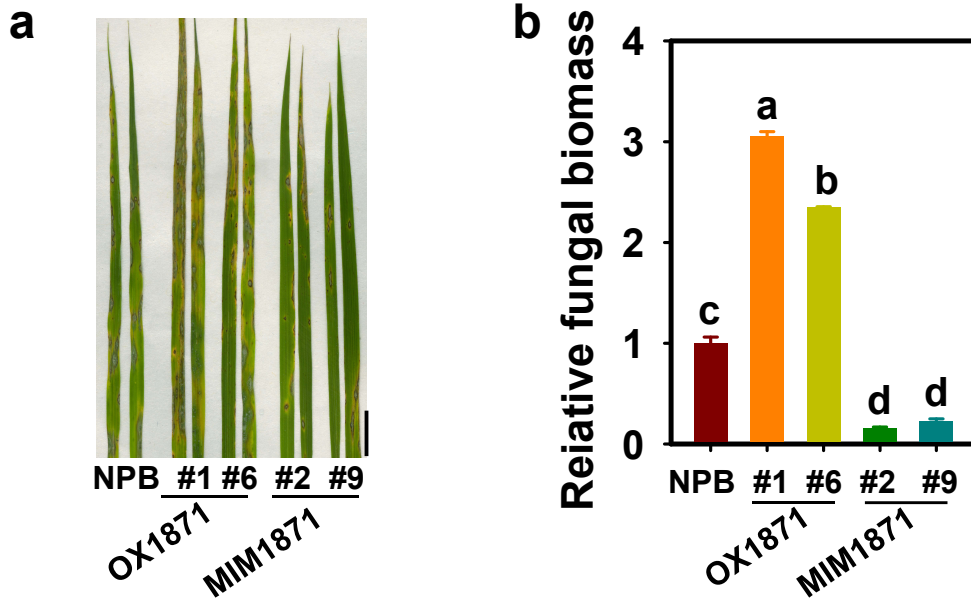
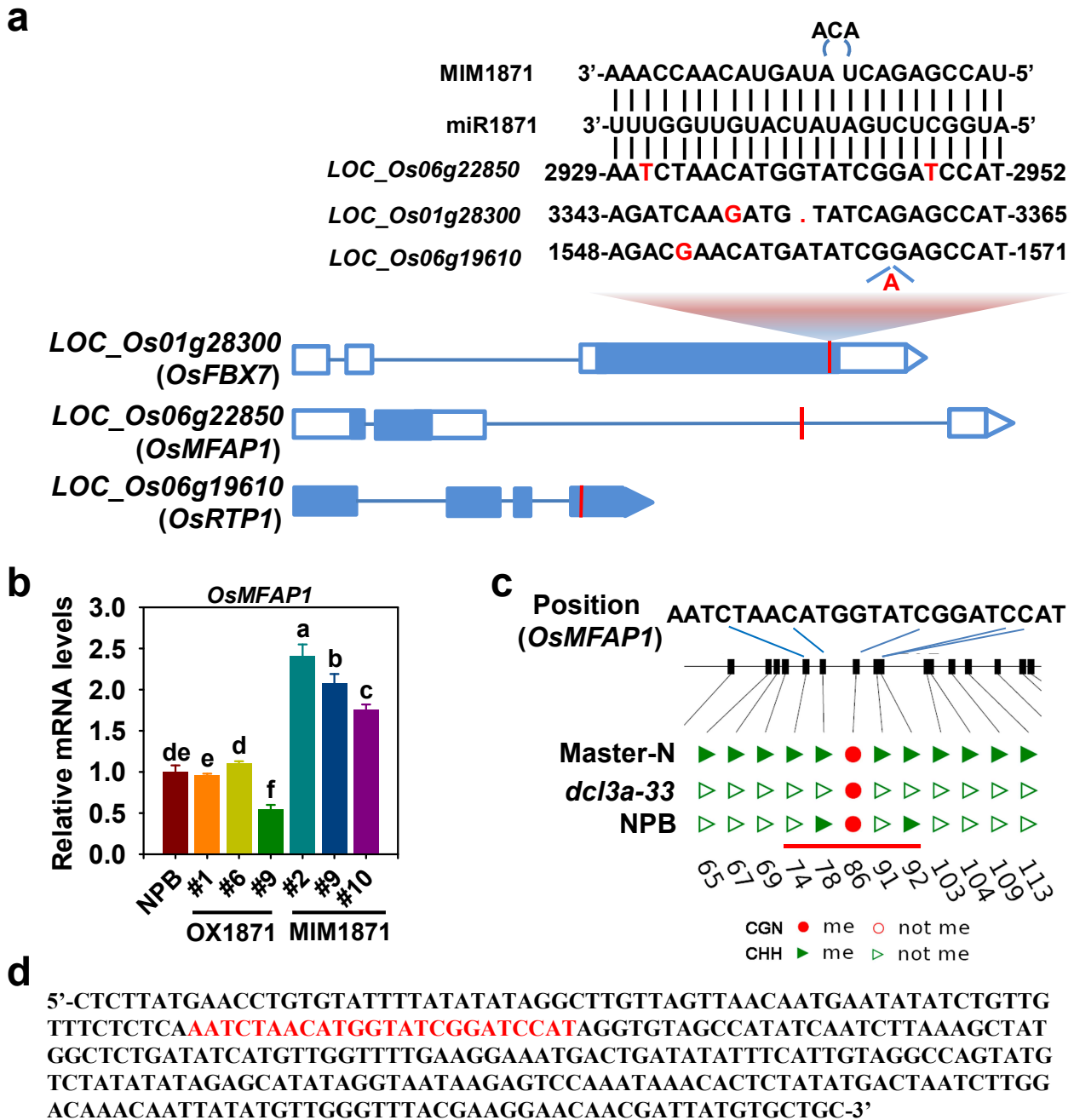


**Figure S1** miR1871 is responsive to rice blast fungus *Magnaporthe oryzae*. The amounts of miR1871 in LTH and IRBLKm-Ts with or without the inoculation of *M. oryzae* isolate GZ8. The miRNA levels were detected by quantitative reverse transcription polymerase chain reaction (qRT-PCR). Data are shown as mean  $\pm$  SD (n = 3 independent repeats). Different letters above the column showed a significant difference ( $P < 0.01$ ) via the One-way Tukey-Kramer test. This experiment was repeated two times with similar results.



**Figure S2** Blocking miR1871 enhances rice resistance against *Magnaporthe oryzae* following spray-inoculation. (a) The disease lesions on leaves of OX1871, MIM1871, and the Nipponbare (NPB) control following spray-inoculation with *M. oryzae* isolate GZ8. The phenotype was captured five days post-inoculation. Scale bars, 1 cm. (b) The fungal biomass in (a). The relative fungal biomass was shown as a ratio of DNA level of *M. oryzae* MoPot2 genes against DNA levels of rice ubiquitin gene. Data are shown as mean  $\pm$  SD (n = 3 independent repeats). Different letters above the column indicate a significant difference ( $P < 0.01$ ) as determined by the One-way Tukey-Kramer test. These experiments were repeated two times with similar results.



**Figure S3** miR1871 is predicted to regulate the methylation of *MFAP1* in rice. (a) The sequence alignment of miR1871 and the target sites of three predicted target genes. Mismatched nucleotides were highlighted in red colors. (b) Reverse transcription quantitative polymerase chain reaction (RT-qPCR) showing the mRNA levels of *MFAP1* in OX1871, MIM1871, and the Nipponbare control. Data are shown as mean  $\pm$  SD ( $n = 3$  independent samples). Different letters above the bars indicate a significant difference ( $P < 0.01$ ) as determined by the One-way Tukey-Kramer test. These experiments were repeated two times with similar results. (c) The cytosine methylation pattern matrix of the DNA fragment of *MFAP1* containing the target site in the *dcl3a* mutant and the Nipponbare control. The open red circles and green triangles represent non-methylated cytosines of CGN and CHH respectively; the solid red circles and green triangles represent methylated cytosines of CGN and CHH respectively. The numbers indicate the site of cytosine in the examined sequence (d). The red line from 74 to 92 indicates the miR1871 target site shown in (d). (d) The DNA fragment of *MFAP1* used to examine DNA methylation in (c). The target site of miR1871 is signed in red.



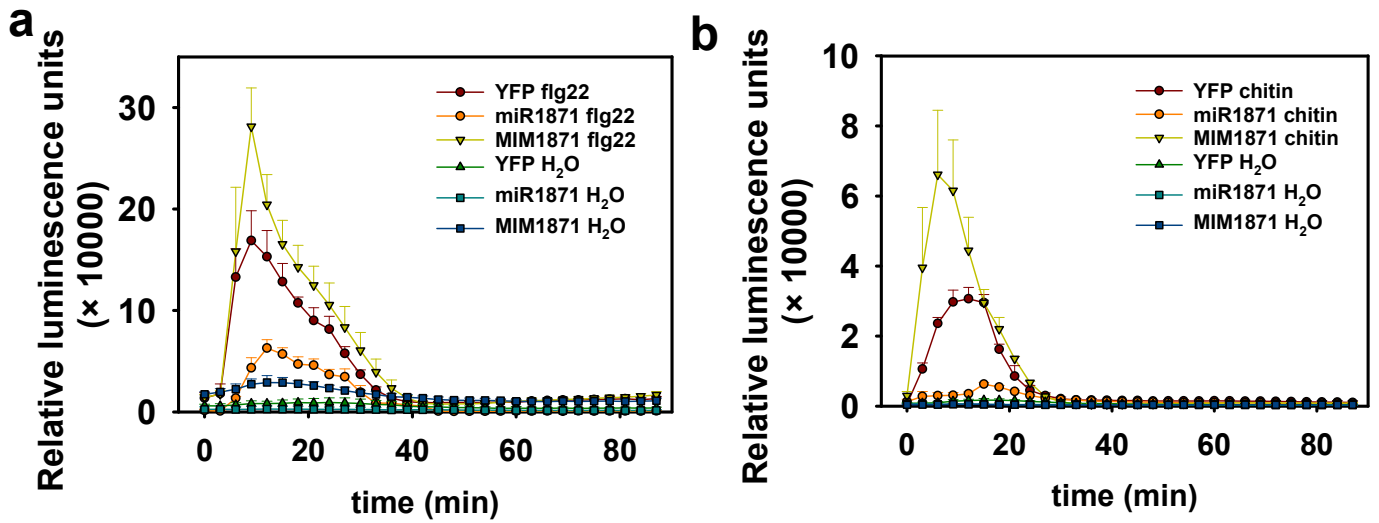


**Figure S5** miR1871 regulates PAMPs-induced Burst of reactive oxidative species (ROS). (a-b) The burst of reactive oxidative species (ROS) induced by flg22 (a) and chitin (b) in the leaves of *Nicotiana benthamiana* transiently expressing miR1871, MIM1871, and YFP, respectively. Data are shown as mean  $\pm$  SD (n = 6 independent repeats).

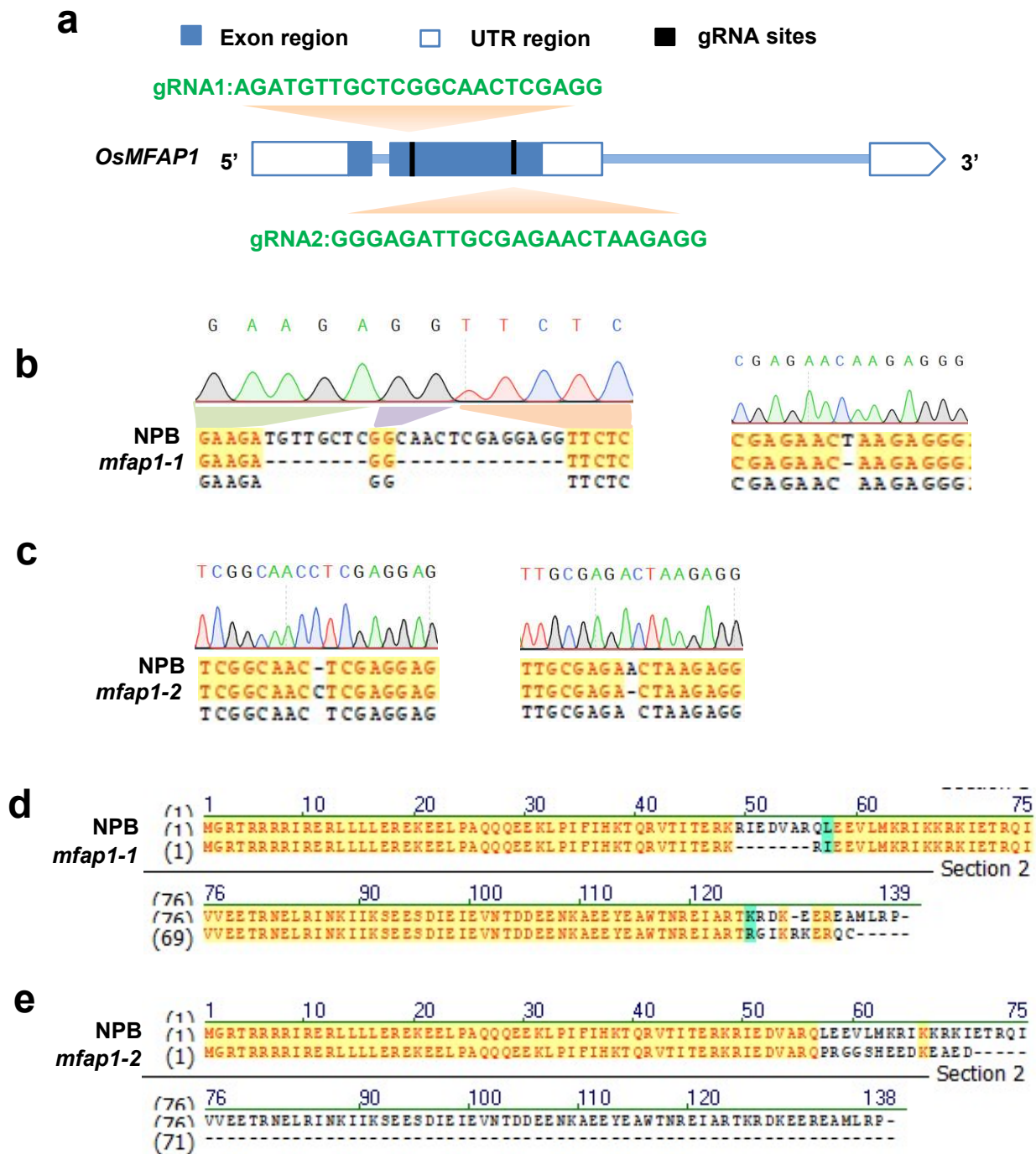


**Figure S6** Mutation sites of MFAP1 in *mfap1* mutants. (a) The sites of guide RNA sequences of MFAP1 gene. (b-c) Alignment of the genomic sequences of mutants *mfap1* with that of the Nipponbare control. (d-e) Alignment of the sequences of the protein of mutants *mfap1* with that of the Nipponbare control.

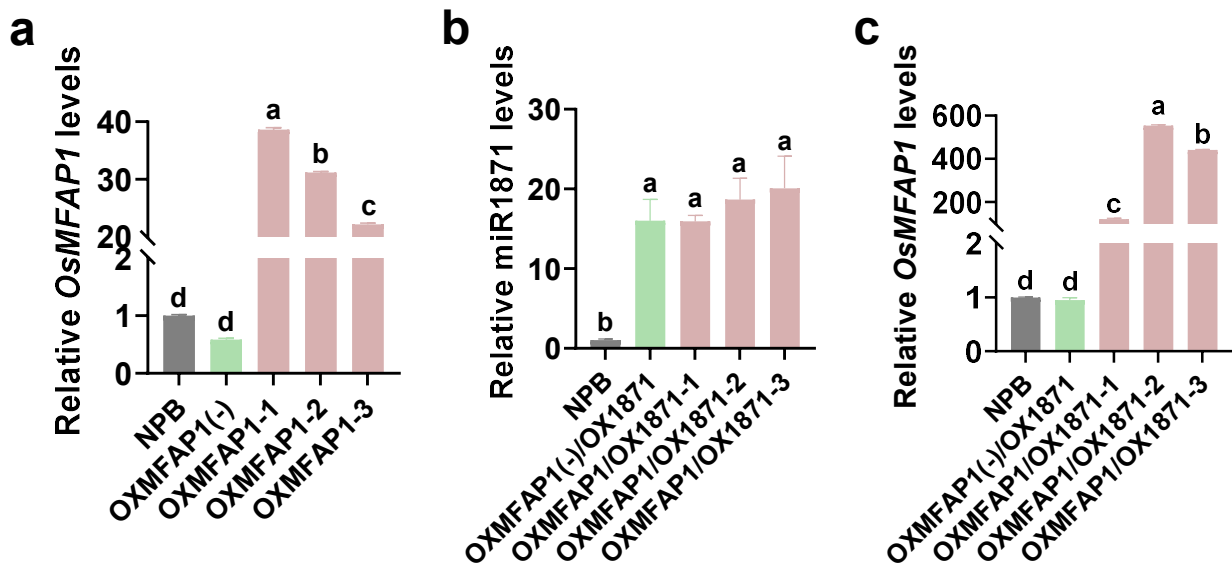


**Figure S7** Overexpression of MFAP1 in the Nipponbare background and OX1871 background, respectively. (a) The mRNA levels of *MFAP1* in the transgenic lines overexpressing the *MIR1871* gene (OXMFAP1), the segregant (OXMFAP1(-)), and the Nipponbare (NPB) control. (b) The amounts of miR1871 in the transgenic lines overexpressing *MFAP1* and *MIR1871* gene (OXMFAP1/OX1871), the segregant (OXMFAP1(-)/OX1871), and the Nipponbare (NPB) control. (c) The mRNA levels of *MFAP1* in the transgenic lines overexpressing *MFAP1* and *MIR1871* gene (OXMFAP1/OX1871), the segregant (OXMFAP1(-)/OX1871), and the Nipponbare (NPB) control.

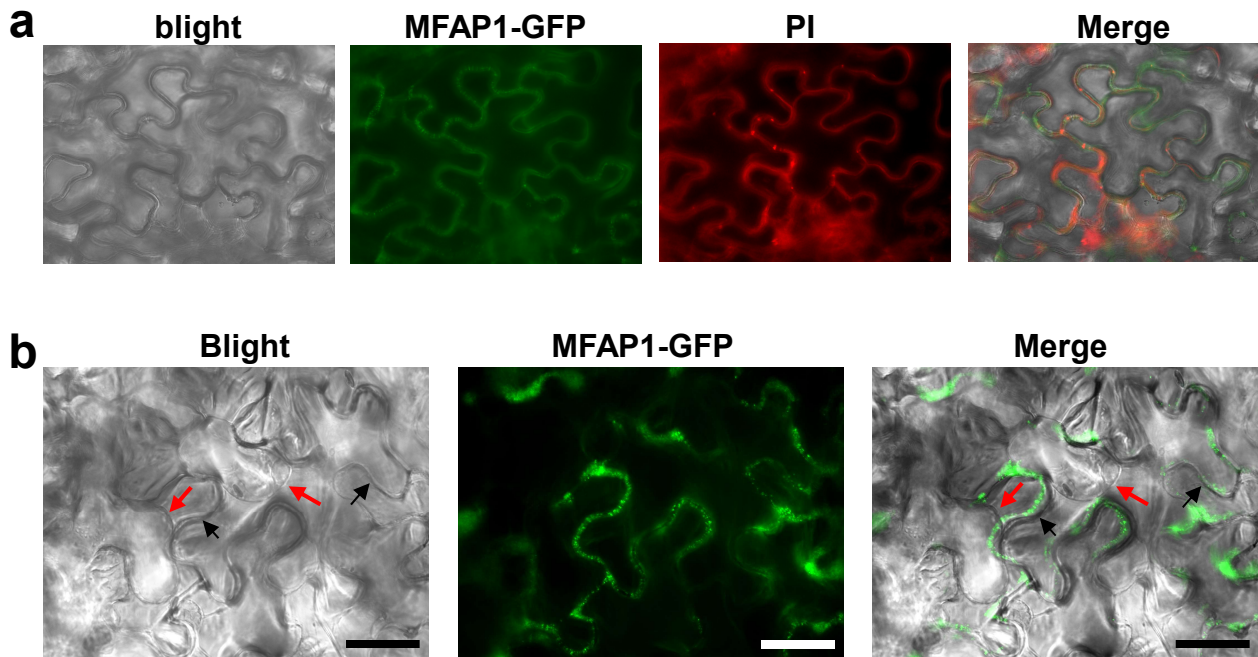


**Figure S8** *MFAP1* is located nearby the cell wall. (a) Colocalization analysis of YFP-tagged *MFAP1* expressed from 35S promoter and cell wall dyed by Propidium Iodide (PI) in *Nicotiana benthamiana*. Bar, 40  $\mu\text{m}$ . (b) the plasmolysis assay showing the location of YFP-tagged *MFAP1* in *Nicotiana benthamiana*. The leaves of *N. benthamiana* were observed after treatment with 0.5 M NaCl for 3 minutes. Bar, 40  $\mu\text{m}$ . The red arrows indicated the cell membrane. The black arrows indicated the cell wall.

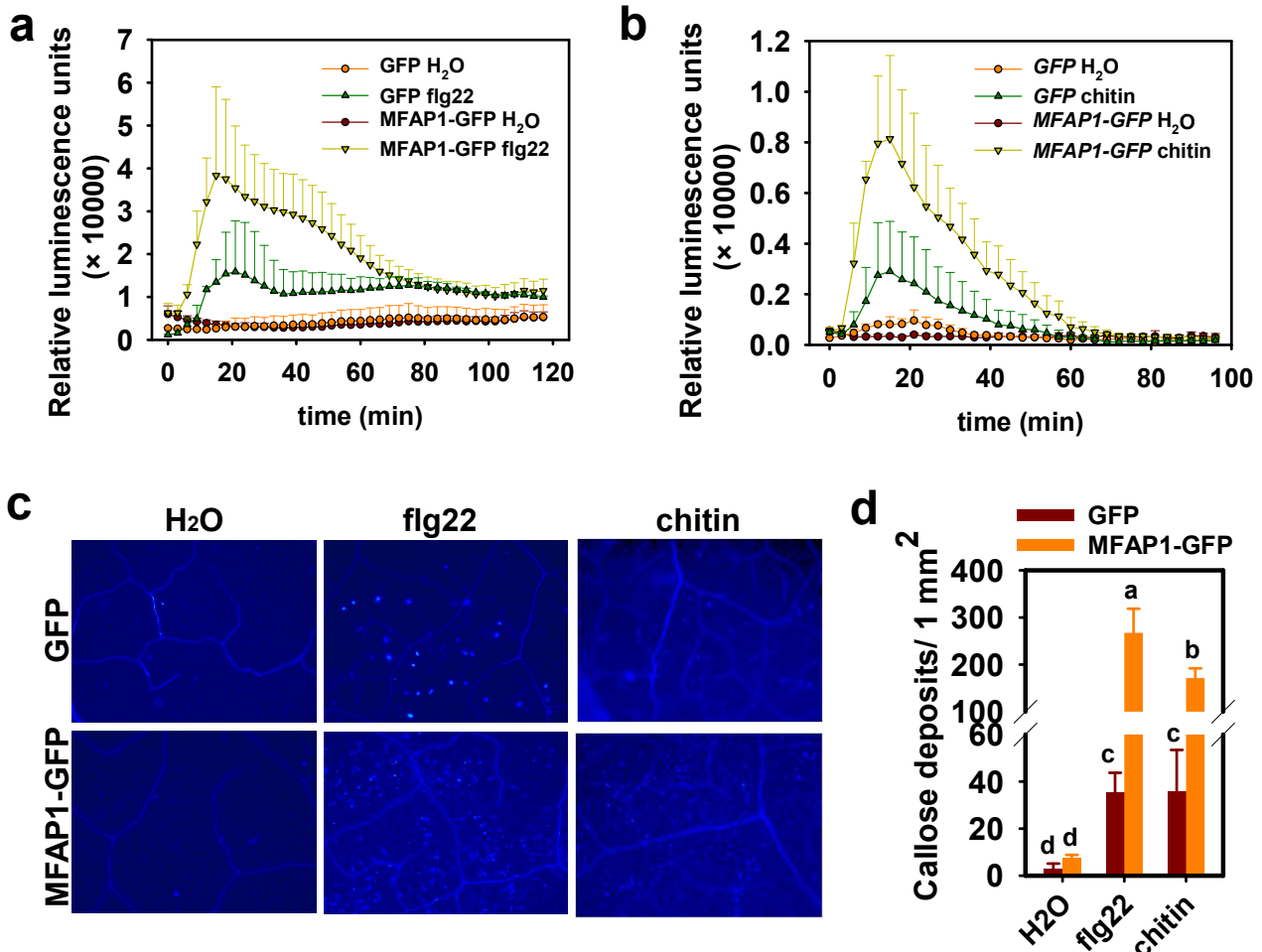


**Figure S9** *MFAP1* positively regulates PTI responses. (a-b) The burst of reactive oxidative species (ROS) induced by flg22 (a) or chitin (b) in the leaves of *N. benthamiana* transiently expressing YFP-tagged *MFAP1*, or YFP alone, respectively. Data are shown as mean  $\pm$  SD (n = 6 independent repeats). (c) PAMPs (flg22 and chitin)-induced callose deposition in the leaves of *N. benthamiana* transiently expressing YFP-tagged *MFAP1*, or YFP alone. Bar, 0.5 mm. (d) Quantitative analysis of PAMPs-induced callose deposition in (c). Data are shown as mean  $\pm$  SD (n = 6 independent repeats). These experiments were repeated two times with similar results.